Parasitology International 67 (2018) 444–453

Contents lists available at ScienceDirect

Parasitology International

journal homepage: www.elsevier.com/locate/parint

Characterization of multiple enolase genes from *Trichomonas vaginalis*. Potential novel targets for drug and vaccine design

Elibeth Mirasol-Meléndez[a], Luis G. Brieba[b], Corina Díaz-Quezada[b], Marisol López-Hidalgo[a], Elisa E. Figueroa-Angulo[c], Leticia Ávila-González[c], Rossana Arroyo-Verástegui[c], Claudia G. Benítez-Cardoza[a,*]

[a] *Laboratorio de Investigación Bioquímica, Doctorado en Ciencias en Biotecnología, ENMyH-Instituto Politécnico Nacional, Guillermo Massieu Helguera No. 239, La Escalera Ticomán, 07320 Ciudad de México, Mexico*

[b] *Laboratorio Nacional de Genómica para la Biodiversidad, Centro de Investigación y de Estudios Avanzados del Instituto Politécnico Nacional, Apartado, Postal 629, 36500 Irapuato, Guanajuato, Mexico*

[c] *Departamento de Infectómica y Patogénesis Molecular, Centro de Investigación y de Estudios Avanzados del Instituto Politécnico Nacional, Av. IPN No. 2508, Col. San Pedro Zacatenco, 07360 Ciudad de México, Mexico*

ARTICLE INFO

Keywords:
Enolase
Trichomonas vaginalis
Gene expression
Glycolytic enzyme
Moonlighting protein

ABSTRACT

Trichomonas vaginalis is the protist parasite that causes the most common, non-viral sexually transmitted infection called trichomonosis. Enolase is a moonlighting protein that apart from its canonical function as a glycolytic enzyme, serves as a plasminogen receptor on the cell surface of *T. vaginalis* and, in consequence, it has been stablished as a virulence factor in this parasite. In the *Trichomonas vaginalis* sequence database there are nine genes annotated as enolase. In this work, we analyzed these genes as well as their products. We found that seven out of nine genes might indeed perform enolase activity, whereas two genes might have been equivocally identified, or they might be pseudogenes. Furthermore, a combination of qRT-PCR and proteomic approaches was used to assess, for the first time, the expression of these genes in the highly virulent mexican isolate of *T. vaginalis* CNCD-147 at different iron concentrations. We could find peptides corresponding to enolases encoded by genes TVAG_464170, TVAG_043500 and TVAG_329460. Moreover, we identified two distinctive characteristics within enolases from *Trichomonas vaginalis.* One of them corresponds to three key substitutions within one of the loops of the active site, compared to host enolase. The other, is a unique N-terminal motif, composed of 15 to 18 residues, on all the potentially active enolases, whose function still has to be stablished. Both differential features merit further studies as potential drug and vaccine targets as well as diagnosis markers. These findings offer new possibilities to fight trichomonosis.

1. Introduction

Trichomonosis is the most-common non-viral sexually transmitted infection caused by the parasitic protozoan *Trichomonas vaginalis*, with > 300 million cases annually worldwide [1]. A distinctive characteristic of *T. vaginalis* is that its genome harbors multiple paralogous copies for a wide majority of genes [2,3]. It is thought, that this genetic multiplicity provides to the parasite the ability to respond to drastic environmental changes (e.g., temperature, microflora, pH, iron concentration, polyamines, zinc, host immune responses, and other unknown factors), by modulating the expression of multiple genes [2,4]. Particularly, since *T. vaginalis* relies on fermentative carbohydrate catabolism, several copies of genes encoding for glycolytic enzymes have been retained during the evolution of this parasite. That is the case of enolase, whose canonical function is the reversible dehydration of 2-phosphoglycerate to phosphoenolpyruvate, the ninth and penultimate step of glycolysis [5]. In addition, this enzyme has been described as a moonlighting protein, in *T. vaginalis* serving as a plasminogen receptor on the cell surface of the parasite [6]. Due to this novel function and location within *T. vaginalis*, enolase has been stablished as a new surface-associated virulence factor. The overall scaffold of this enzyme is very similar among several organisms [7], but its sequence is moderately conserved [8] and it is possible to find important differences between pathogenic and host enzymes. In consequence, enolase has been proposed as an attractive target for drug discovery and vaccine development in several pathogens like *Toxoplasma gondii*, *Leptospira spp.*, and Trypanosomatid parasites, among others [9–12]. Furthermore, novel strategies to treat physiopathologies like cancer and type 2 diabetes

* Corresponding author.
E-mail address: beni1972uk@gmail.com (C.G. Benítez-Cardoza).

https://doi.org/10.1016/j.parint.2018.04.003
Received 4 August 2017; Received in revised form 10 March 2018; Accepted 11 April 2018
Available online 14 April 2018

mellitus (and comorbidities) have targeted the moonlighting (non-glycolytic) functions of enolase [13,14]. In TrichDB database (www.trichdb.org) there are 9 gene-sequences explicitly annotated as enolase [15,16], but they have not been fully characterized. Here we used a combination of bioinformatics, molecular and proteomic approaches to characterize the sequence and expression of enolase genes in *Trichomonas vaginalis* genome. This information contributes in identifying novel drug and vaccine strategies to combat trichomonosis.

2. Materials and methods

2.1. Database mining and genome analysis of expressed sequence tags (EST)

An alignment of protein enolases from *T. vaginalis* sequences found of TrichDB (www.trichdb.org) were made in order to identify non redundant sequences. Furthermore, in the alignment enolase sequences from other organisms were included. The alignment was made with CLUSTALW (http://www.ebi.ac.uk/Tools/msa/clustalw2/). In this manuscript, we indicate the position of each residue in the sequence of each enolase and also, to have a common reference, the position of that same residue (in parenthesis and bold) according to the sequence of *S. cerevisiae* enolase, indicated at the top of this alignment [5]. The sequences were qualified with SeaView [17], and sequences were aligned with Muscle [18]. Manual corrections and phylogenetic reconstruction were performed with PhyML [19] using GTR (Generalized time reversible) as a substitution model and a Bootstrap of 1000. Clustering was performed with a 97% threshold using Mothur [20].

2.2. Parasite growth

Parasites of *T. vaginalis* clinical isolate CNCD-147 [21] were cultured in trypticase–yeast extract–maltose (TYM) medium supplemented with 10% heat inactivated horse serum and incubated at 37 °C for 24 h. The parasites were maintained in in vitro cultures for up to 2 weeks. To obtain iron depleted conditions, TYM medium was complemented with 100 μM of 2-2′ dipyridyl (Sigma). To get normal or high iron concentration, TYM medium was supplemented with ammonium ferrous sulfate 20 μM or 250 μM (JT Baker) respectively, 24 h before parasite culture started.

2.3. Cloning, overexpression and purification of TVAG_329460

The ORF of gene identified as TVAG_329460 was amplified from genomic DNA of *T. vaginalis*. The PCR primers were 5′ aac ggg aat cat atg aac gcc gag cac gac - 3′ (forward) and 5′ gag gac gga tcc tta ttc ctc agc gag cat gtc -3′ (reverse). The PCR product was cloned into the *Nde*I and *Bam*HI restriction sites (underlined) of a modified pET19 vector (Courtesy of Professor Tom Ellenberger, Washington University School of Medicine). Positive clones of TVAG_329460 were confirmed by automated DNA sequencing. The plasmid pET19:TVAG_329460 was used to transform *E. coli Rosetta II,* and plated onto an agar plate supplemented with 100 μg/mL ampicillin and 34 μg/mL chloramphenicol. A single colony was used to grow a 100 mL overnight LB culture complemented with the same antibiotics, which was used to inoculate a 2 L culture in 2× YT medium. This culture was grown at 37 °C, until OD_{600} reached a value of 0.6. Recombinant protein expression was induced by adding 1 mM IPTG and cultures were incubated for five hours. Cells were harvested by centrifugation and frozen at −80 °C, until used. Pellet was re-suspended in lysis buffer (20 mM Imidazole, 50 mM Tris-HCl, 300 mM KCl, 0.02 2-mercaptoethanol, 20% glycerol, 0.01 M PMSF and 0.1 mg lysozyme, pH 8.0), and bacteria were lysed by sonication. Cell debris was removed by centrifugation at 10000*g* for 30 min at 4 °C. Enolase was purified using Ni-Sepharose High performance (GE Healthcare). This column was equilibrated with buffer A (20 mM Imidazole, 50 mM Tris-HCl and 300 mM KCl, pH 8.0). The contaminant proteins were eliminated by washing with 10 column-volumes of buffer A. Enolase was eluted with three column-volumes of buffer B (500 mM Imidazole, 50 mM Tris-base and 300 mM KCl, pH 8.0). Purified protein was extensively dialyzed against cleavage buffer (20 mM Tris-HCl, 50 mM NaCl, 1 mM DTT, 2 mM EDTA, pH 8.0). The histidine tag was cleaved by the addition of 0.1 mg PreScission Protease (GE Healthcare) per 10 mg of purified protein. Enolase was further purified by ion exchange chromatography on a Hitrap Q HP column (GE Healthcare). In this case, the equilibration buffer was, (50 mM Tris-HCl, 1 mM EDTA, 2 mM DTT, pH 8.0) and the elution was carried out using a gradient from 0 to 1 M NaCl. The enzymatic activity of purified enolase was confirmed by the coupling reaction to pyruvate kinase and lactate dehydrogenase and following the decrease of NADH absorbance at 340 nm, as described early [22].

2.4. Polyclonal antibodies

Female New Zealand white rabbits weighting 3.0 kg were intramuscularly immunized twice with 300 μg affinity-purified enolase TVAG_329460 protein in a 1:1 ratio with TiterMax Gold (Sigma) adjuvant, as recommended by the manufacturer. The animals were bled weekly, and their sera were tested by WB assays against recombinant protein. Before rabbit immunization, the preimmune serum was obtained from each rabbit and used as a negative control for all experiments with antibodies.

2.5. Total protein extracts

Logarithmic-phase parasites growth either at low, normal and high iron conditions (0, 20 and 250 μM) were washed three times with cold PBS pH 7.0. Afterwards, 2×10^7 parasites were resuspended in 0.9 mL of cold PBS pH 7.0 and 0.1 mL of 100% TCA, mixed well and incubated for 18 h at 4 °C. Subsequently, cells were centrifuged at 12,000 ×*g* for 3 min at 4 °C. The pellet was washed five times with cold PBS pH 7.0, centrifuged at 12,000 ×*g* for 5 min at 4 °C and washed once more with cold acetone, followed by centrifugation. The pellet was resuspended in 400 μL of 1× sample buffer (BM 1×) with 5% β-mercaptoethanol and boiled for 3 min, centrifuged at 12,000 ×*g* for 3 min and loaded from 100 to 200 μL of the sample in preparative gels of polyacrylamide for 2DE and 15 μL for SDS-PAGE.

2.6. SDS PAGE and western blot analysis

SDS-PAGE were performed using total protein extracts from 20 million of *T. vaginalis* parasites at acrylamide gels SDS-PAGE at 8% which was stained with Coomassie blue G250. For Western Blot analysis, proteins were transferred from gels to polyvinyldifluoride (PVDF) membranes that were blocked using Blot-Quickblocker solution (Millipore) in PBS buffer complemented with 0.05% of Tween 20 (PBS-T) for 18 h at 4 °C. The membranes were washed five times with PBS-T at 25 °C and incubated for 2 h at 4 °C with polyclonal antibody anti-enolase TVAG_329460. The antibody was diluted in PBS-T at a 1:5000 ratio. The membrane was washed five times with PBS-T at 25 °C, incubated with secondary antibody (α-rabbit immunoglobulin G [IgG] coupled to peroxidase) (Bio-Rad) at a 1:3000 dilution in PBS-T for 2 h at 25 °C, washed five times with PBS-T, and developed with 3,3-Diaminobenzidine (Sigma). All experiments were done by triplicate.

2.7. 2-DE and Western blot analysis

2-DE assays were performed using total protein extracts from 20 million of *T. vaginalis* parasites using low, normal and high iron conditions (0, 20 and 250 μM) as indicated before. For the first dimension, total protein extracts in rehydration solution (BioRad) were loaded onto a 7 cm ready-immobilized pH gradient (IPG) strips (linear pH gradient 3–10; BioRad). IPG strips were actively rehydrated for 16 h at 4 °C.

Isoelectric focusing (IEF) of proteins was performed in three steps: 250 V for 20 min, 4000 V for 3 h, and a gradual increase to reach 10,000 V in one hour. For reduction and alkylation, strips were equilibrated in Buffers I and II (BioRad) for 10 min at room temperature each. Subsequently, the proteins were transferred to acrylamide gels SDS-PAGE at 12% which were stained either with silver stain or Coomassie Blue G-250. After 2-DE, proteins were transferred onto nitrocellulose membranes and blocked using 10% fat-free milk in PBS-T buffer for 18 h at 4 °C; afterwards they were washed five times with PBS-T at 25 °C and incubated for 18 h at 4 °C with polyclonal antibody anti-enolase TVAG_329460. The nitrocellulose membranes were washed five times with PBS-T at 25 °C, incubated with secondary antibody (α-rabbit IgG coupled to peroxidase) for 2 h at 25 °C, washed five times with PBS-T, and developed with 4-chloro-1-naphthol (Bio-Rad). The corresponding pre-immune rabbit serum was used as negative control. Gels and nitrocellulose membranes were analyzed using the Quantity One software (BioRad) and PDQuest software (BioRad). The western blot, allowed us to identify the spots corresponding to enolase for further analysis. All experiments were independently performed at least three times, using independent parasite cultures and yielded similar results.

2.8. Identification of proteins

Protein spots of interest that were previously excised from Coomassie Blue G-250 stained gels, were treated to allow tryptic digestion and analyzed by Matrix assisted lasser desorption/ionization (MALDI)- time of Flight (ToF) Mass spectrometry as previously described [23,24] (Department of Biotechnology and Biochemistry, CINVESTAV, Unidad Irapuato). Protein identification was performed by searching the NCBInr database and the draft of the *T. vaginalis* genome sequence from the TrichDB web page (http://trichdb.org/trichdb/).

2.9. Real -time PCR

RNA was extracted by TRIzol method following manufacturer's recommendations from parasites grown as described above. RNA purity and concentration were tested by the ratio of absorbances at 260/280 nm using a Thermo Scientific NanoDrop 1000 Spectrophotometer. The primer sets were 20 nucleotides-length and were designed to amplify fragments from 200 to 300 bp using TrichDB sequences for eight out of nine enolase genes (the gene TVAG_148010, was not considered for this analysis, since it has not any EST reports) and tested by OligoAnalizer 3.1-Integrated DNA Technologies (https://www.idtdna.com/calc/analyzer). Sequences and Tm for each pair of primers used are described (Table 1). qRT-PCR was performed using specific primers for each gene and KAPA SYBR FAST Universal One-Step qRT-PCR kit. The reactions were carried out in an Applied Biosystems Step One ™ Real-Time PCR System. β-Tubulin was used as internal control. All genes were amplified using 30 cycles of three steps; denaturation (94 °C for 30 s), annealing (Tm of each primer pair for 30 s) and elongation (72 °C for 30 s). Quantitative analysis of the genes in different independent triplicates were done by comparative Ct method ($2^{-\Delta\Delta Ct}$, $\Delta Ct = Ct_{tub} - Ct_{ENO}$, $\Delta\Delta Ct = \Delta Ct_{sample} - \Delta Ct_{control}$) [25]. Fold changes in mRNA levels (mean SD) are expressed relative to enolase gene TVAG_464170 at normal iron conditions.

Table 1
Primers for PCR amplification were designed using mRNA sequence for each gene annotated as enolase from *T. vaginalis*.

Gene ID	Primers sequences	
	Forward	Reverse
TVAG_329,460	5′-gcgaactcgactacgagaac-3′	5′-taataataaatcaggaaaga-3′
TVAG_043500	5′-ttaaccagatcggtacaatc-3′	5′-tcatagaagtttactcctca-3′
TVAG_464170	5′-atgagtgttcagcaagtatt-3′	5′-cgcggccaacaaccttctcg-3′
TVAG_358110	5′-gaattaaacgaagagccact-3′	5′-tgttgagtaatggtgcaaaa-3′
TVAG_263740	5′-atgtcagctgataaggttgc-3′	5′-agcaagatcttctggcttct-3′
TVAG_487600	5′-taacccagccaagtaccaat-3′	5′-cttcgtacatgtttggaatg-3′
TVAG_170370	5′-aaaaatccgcaattctttcg-3′	5′agaaccgataattccacctc-3′
TVAG_282090	5′-ggggcagctattagacatga-3′	5′-tgctcaggaaagctgatatc-3′

3. Results

In this work, all genes are named according to their identification in TrichDB. It is worth to mention that all nine enolases are also reported in NCBI protein database. In Table S1, we show, the nomenclature used in NCBI. Nevertheless, in this manuscript these identification numbers or names are not used, to avoid any confusion.

3.1. Genomic organization of genes annotated as enolase in T. vaginalis genome

Before 2014, in TrichDB (http://trichdb.org/trichdb/) there were 19 non-redundant sequences related to enolase. However, in 2014 the data base was refined and now, only nine sequences are annotated as enolase. An in silico analysis revealed that these nine sequences are independent genes, because they belong to different contigs. Some characteristics of each of these genes like contig, position, number of bp of the genomic and coding sequences, polarity, number of aminoacid residues and nucleotides, isoelectric point, and adjacent genes, both up and downstream are shown in Table S1.

In TrichDB some sequences of genes encoding for enolases have annotated their 5′or 3′UTR sequences, or both, but not all of them. Therefore, we examined 50 bp upstream (panel a) and downstream (panel b) from initiation (ATG) and stop (TAA) codons for all enolase genes.

Concerning 5′UTR, it has been reported that about 75% of the upstream sequences of protein coding genes within *Trichomonas vaginalis* contain a metazoan initiator-like element (Inr) [26]; described as motif I and with ~80% being located at positions −6 to −20 relative to the start codon, whose highly conserved sequence is TCA + 1Py(T/A). Motif I is found in all enolase genes and highlighted in Fig. 1 panel a. Some genes (TVAG_464170, TVAG_263740, TVAG_487600 and TVAG_282090) show two putative Inr (motif I) elements. In addition to motif I, four other sequences (motifs II–V) have also been identified in the 5′-upstream region of *T. vaginalis* genes [26,27]. Some of these motifs could be identified in the upstream regions of initiation codons (Fig. 1 panel a). It has been reported that motif II, is frequently encountered 20–40 bp upstream of the start codon and around 15 bp upstream of motif I [26]. In enolase genes, all sequences show the presence of motif II. It is to note that, genes TVAG_464170, TVAG_282090 and TVAG_148010 show motif II downstream from motif I. Regarding motif III, it has been found commonly at −40 to −80 bp relative to the start codon. In the case of enolase genes, the sequences corresponding to TVAG_464170, TVAG_263740 and TVAG_487600 also show motif III. Only TVAG_464170 displays this motif downstream motif I. In the case of Motif IV it could be found in enolase genes TVAG_043500, TVAG_263740, TVAG_282090 and TVAG_170370. Motif V was not found in none of the enolase genes.

In addition, the sequence analysis, allowed us to notice that TVAG_464170 might have a different initiation codon, 63 bp downstream to that annotated in TrichDB (Fig. S1). This putative initiation codon, also shows its own Inr element containing putative TSS 14 bp upstream from the putative start codon. If that would be the case, Motifs II and III would be upstream from Motif I, as commonly observed in *Trichomonas vaginalis* genome. The putative initiation codon, matches exactly with the Inr, and initiation codons of the most closely related genes TVAG_043500 and TVAG_329,460. Further work is needed to confirm this new putative position of Inr and start codon of TVAG_464170.

Regarding the 3′UTR sequences (Fig. 1 panel b), we found the

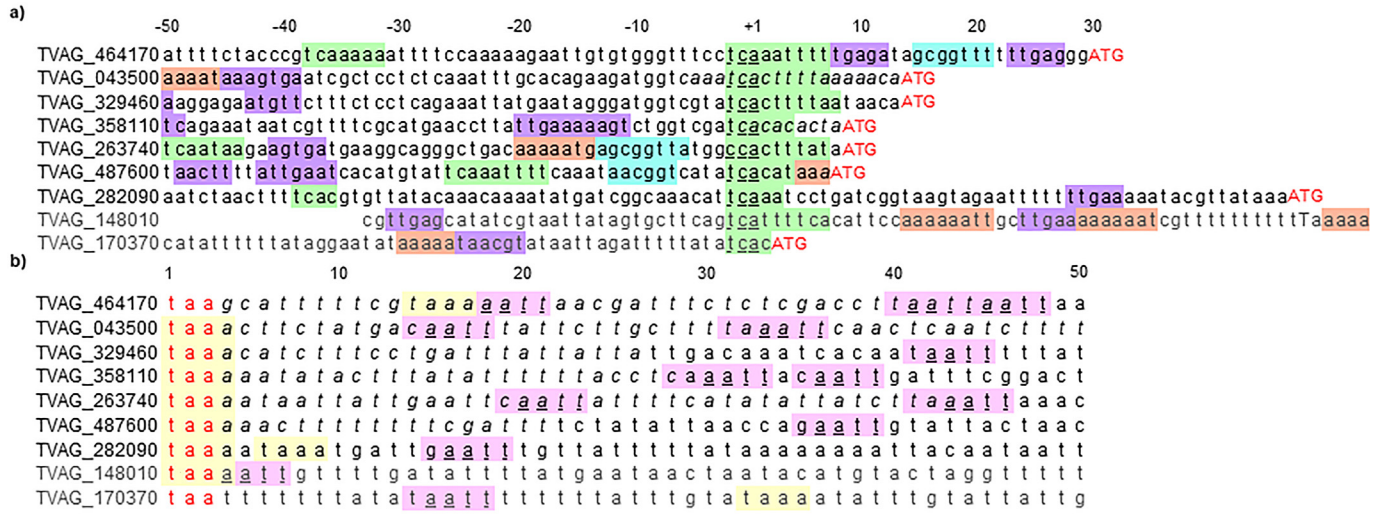

Fig. 1. 5′ (panel a) and 3′ (panel b) non-coding sequences of enolase genes from *T. vaginalis*. In panel a, the nucleotides are aligned by the sequence TCA (underlined) as the putative TSS (A is numbered as +1). The start codons are shown in red capital letters. Core promoter elements are marked as indicated; motif I (green); motif II (purple); motif III (blue) and motif IV (orange). In panel b, sequences are aligned by the stop codon (marked with red letters). The polyadenylation signals are marked in yellow boxes, while the cleavage sites are highlighted in pink. The conserved minimal motif downstream from and adjacent to the cleavage site is shown underlined (AATT). (For interpretation of the references to colour in this figure legend, the reader is referred to the web version of this article.)

highly conserved tetranucleotide with sequence UAAA, as the polyadenylation signal [28,29]. Almost all enolases show UAAA motif overlapping the stop codon, except for TVAG_464170 and TVAG_170370, whereas TVAG_282090 shows two polyadenylation signal motifs. Also, we observed the presence of (U/C/G)↓$(A)_{2\text{-}5}$UU as the cleavage site. All enolase genes show the cleavage site downstream from polyadenylation signals, the only exception is TVAG_170370. The 3′ poly(A) tail of mRNA is involved in regulatory mechanisms such as mRNA stability, export of mRNA from the nucleus to the cytoplasm, and initiation of translation [27].

3.2. Sequence analysis of enolases from Trichomonas vaginalis and other organisms

The aminoacid residues alignment of the nine *T. vaginalis* enolase sequences are shown in Fig. 2. In the same image we also show the sequences corresponding to enolase from *Saccharomyces cerevisiae*, *Human* (isoform alpha), *Entamoeba histolytica* and *Streptococcus pneumoniae,* each of these organisms belong to different phylogenetic order and crystallographic structure reported with PDB ID: 3B97, 3ENL, 3QTP and 1W6T respectively (http://www.rcsb.org).

Regarding, enolases from *T vaginalis*, the identity percentage of aminoacid residues conservation oscillate between 24.15 and 96.19%. In Fig. 3, the phylogenetic tree shows the evolutionary relationships based on the alignment. We observed that seven (TVAG_464170, TVAG_043500, TVAG_329460, TVAG_358110, TVAG_263740, TVAG_487600 and TVAG_282090) out of nine enolase genes could be clustered together, and among them, TVAG_464170, TVAG_043500 are more closely related, followed by 329460. The other four enolases, evolved differently, from the first group. Sequences TVAG_170370 and TVAG_148010, show low relationship from the rest of the enolase genes, since they are the most divergent sequences.

When *T. vaginalis* sequences are compared to enolases from other organisms, we obtained that the products of the seven more similar *T. vaginalis* enolases show identities around 40 to 46%. The other two *T. vaginalis* enolases are less conserved, showing percentages close to 28 of identity.

An outstanding feature of all enolases from *T. vaginalis* is the unique N-terminal extension of 35 to 63 aminoacids residues that is absent in enolases from other organisms. To further explore whether these N-terminal extensions, were conserved in any other organism, we performed local alignment searches for each of the sequences, using several protein databases and algorithms like Blast and HHBlits [30,31]. We found that, the region corresponding to $^{6(-55)}$MSVQQVLKVGLKSGLITLFVAMNAENDAI$^{35(-24)}$, of the product of TVAG_464170 shows 55 and 79% of identity and homology, respectively to chitin synthase from *Tetrahymena thermophila* SB210 (Sequence ID: XP_001019671.2, [32]). We could not find any similarity with proteins from mammals. Due to the low identity and similarity between enolases from *T. vaginalis* and from human, and more particularly, considering the uniqueness of N-terminal extensions observed in *T. vaginalis* enolases, these regions deserve further attention as potential target for drug and vaccine design.

3.3. Functional domains of enolases from T. vaginalis

3.3.1. Analysis of the catalytic and metal binding sites

The catalytic site of enolase from different organisms has been described [7,33–36]. Nevertheless, for mechanism, the enolase from yeast is the best studied, with multiple X-ray structures, mutagenesis and mechanistic studies [37]. From them, seven residues have been implicated in binding substrate and/or participating in catalysis (H160 (160), E169 (169), E212 (212), K346 (346), R375 (375), S376 (376) and K397 (397)) [33]. In addition, the active site of α-human enolase (hENO1) has been described to involve also some loops; L1 ($^{37(37)}$SGASTGIY$^{44(44)}$), L2 ($^{157(159)}$SHAGNKL$^{163(165)}$) and L3 ($^{263(266)}$SPDDPSRYI$^{271(274)}$) [7]. Apart from the catalytic residues, enolase requires to bind a divalent cation (commonly Mg^{2+}) as a cofactor to perform the catalytic event. The residues involved in Mg^{2+} binding reported for hENO1 and other species are E293 (296), D245 (247), D318 (321) and S40 (40) [38–40].

We found that seven sequences (encoded by TVAG_464170, TVAG_043500, TVAG_329460, TVAG_358110, TVAG_263740, TVAG_487600 and TVAG_282090; coincidently the most evolutionary related enolases) contain all seven catalytic residues, all Mg^{2+} binding residues as well as complete L1. Regarding the L2 region we found that the same seven enolases, as well as the product of TVAG_170370, kept four out of seven conserved residues with three non-conservative substitutions K157(159)S, G161(163)N and N162(164)K, when compared with α-human enolase. These key differences on L2 region, might be exploited for searching specific inhibitors of the active site of *T. vaginalis* enolases, and in consequence for the development of new drugs; as

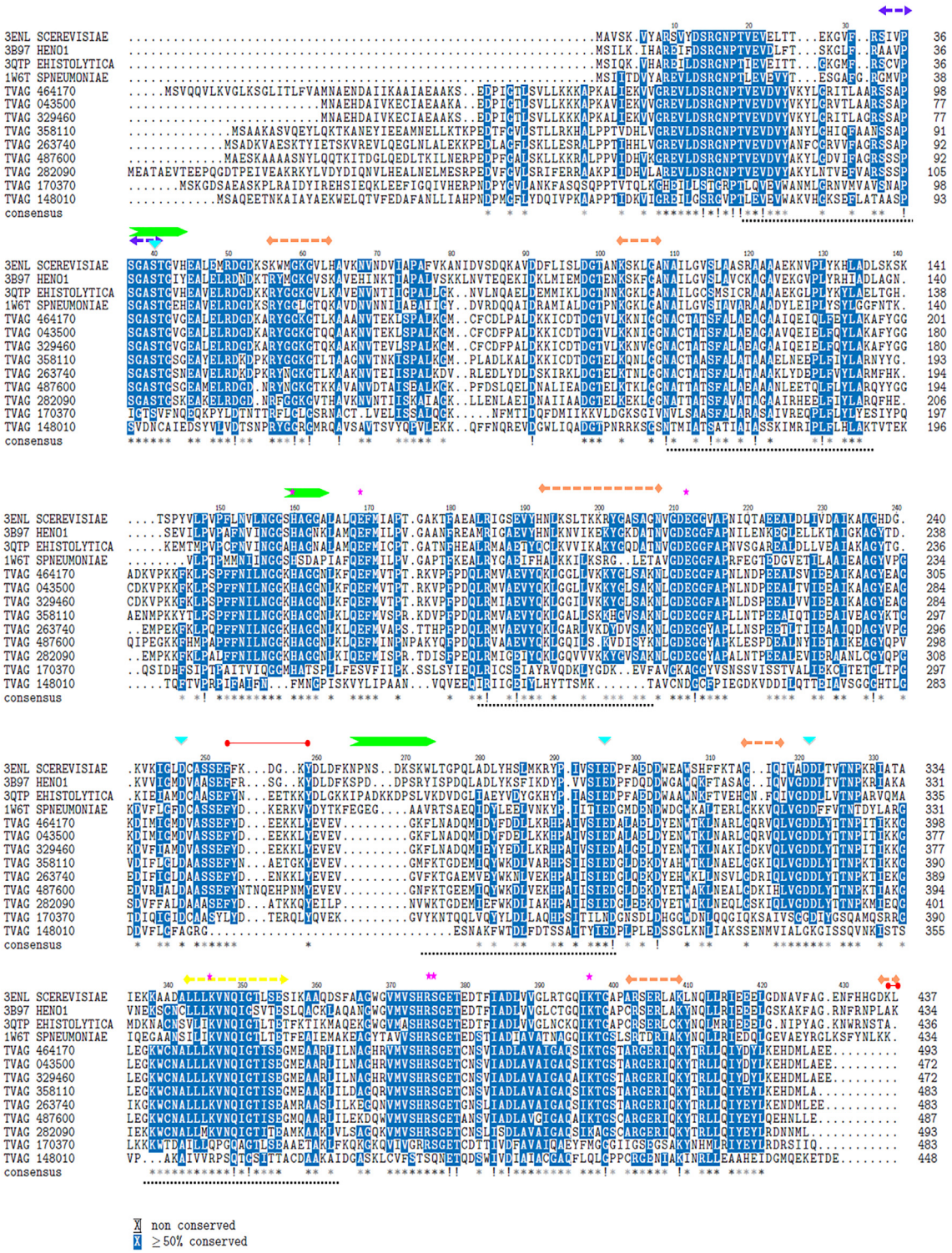

Fig. 2. Protein sequence alignment corresponding to genes annotated as enolases in *T. vaginalis* sequence data base TrichDB and other organisms using CLUSTALW (http://www.ebi.ac.uk/Tools/msa/clustalw2/). Blue indicates conserved regions and white indicates non-conserved regions. Loops of active-site regions are indicated by green arrows and cyan triangles indicate Mg^{2+} binding residues. Catalytic residues are indicated by pink stars. Red bars indicate the plasminogen binding residues, yellow bar indicates the enolase signature, orange bar indicates the RNA binding sites, purple bar indicates the hydrophobic domain and black dotted bar indicates the immunogenic conserved regions. (For interpretation of the references to colour in this figure legend, the reader is referred to the web version of this article.)

it has been proposed for enolase from trypanosomatid parasites [12]. For the product of gene TVAG_148010 we did not find any conserved residues within this loop. Finally, for the region L3, we observed that the loop is non-conserved in enolases from *T. vaginalis* when compared with hENO1; and it is only partially conserved in enolases from other organisms (*E. histolytica, S. cerevisiae* and *S. pneumoniae*). Respect to metal binding residues, the product of gene TVAG_170370 has only two out of four conserved residues, with two no conservative substitutions

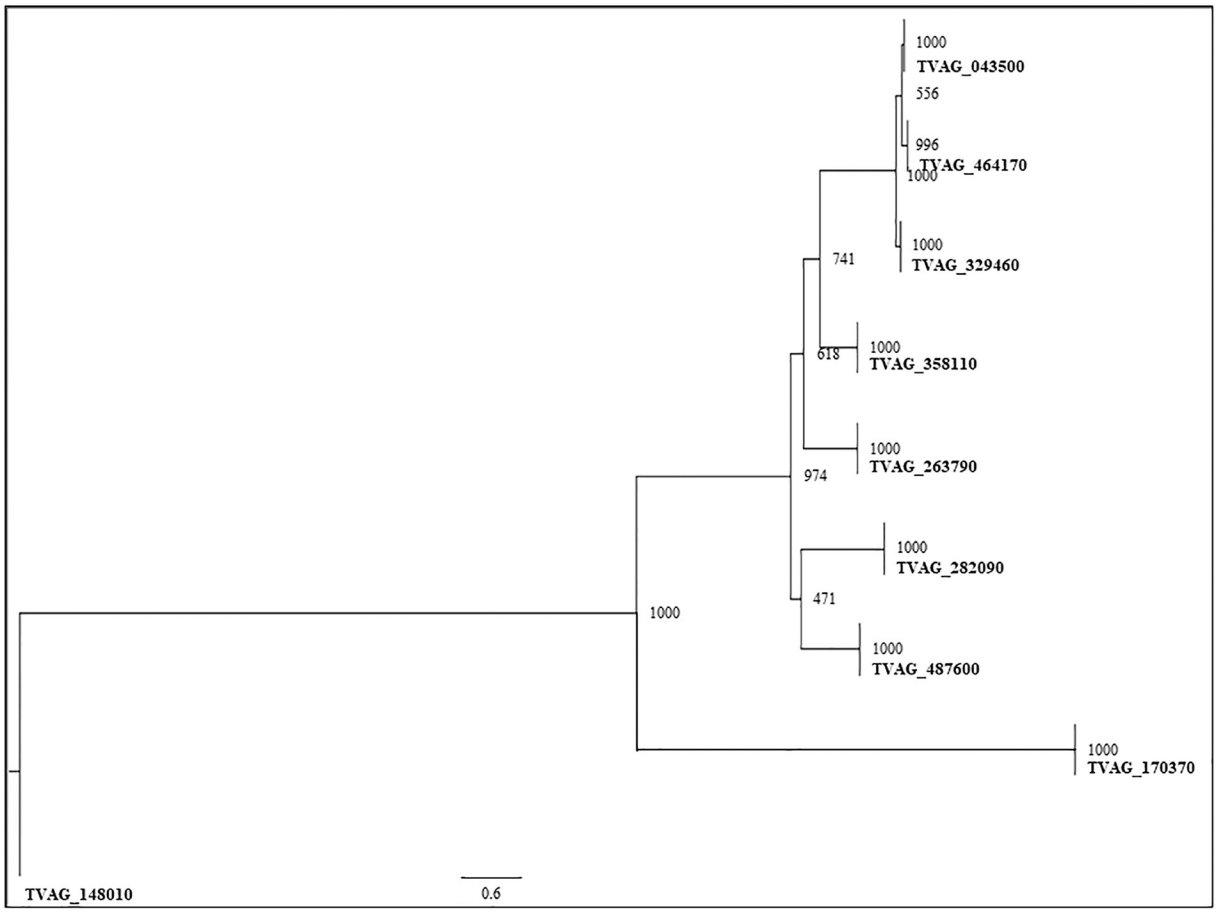

Fig. 3. Phylogenomic reconstruction of enolases from *T. vaginalis.* Reconstruction was performed as described in Materials and Methods section. Maximum likelihood bootstrap percentage support values are indicated.

with respect to *S. cerevisiae* enolase (N/E 293(296) and G/D 318(321). For TVAG_148010 we found only one residue out of four conserved with three non-conservative substitutions with respect to *S. cerevisiae* enolase (N/S 40 (40), A/D 245(247) and G/D 318 (321)) [36].

Therefore, according to the conservation of active sites and divalent cation binding site, enolases corresponding to TVAG_170370 and TVAG_148010, although they might show the enolase signature, and in consequence, they have been annotated as putative enolases, they might not be capable of performing the canonical catalytic reaction of enolase.

3.3.2. Analysis of the plasminogen binding site

Enolase has been found to bind plasminogen on the cell surface within several organisms [5,8,41–43]. In *Trichomonas vaginalis*, enolase encoded by TVAG_329460 [6] has been demonstrated to perform plasminogen binding activity, and in consequence, described as a new virulence factor that deserves further attention.

The best characterization of the plasminogen binding site has been reported for *S. pneumoniae*, by a combination of mutagenesis and binding studies. Two sites have been located [35,43–46]. One of them is known as the C-terminal site and is composed by two lysine residues ($^{433(435)}$KK$^{434(436)}$) at the C-terminal end. In the case of enolases from *Trichomonas vaginalis*, none of them show any of these two lysine residues. Even though this site, is not well conserved in enolases which have confirmed to be capable of binding plasminogen [35,43–46]. The other site, depicted as the internal site, is composed by a nine residue motif ($^{248(253)}$FYDKERKVY$^{256(259)}$) within the sequence of *S. pneumoniae*. This site was thoroughly analyzed for the sequence of *Trichomonas vaginalis* enolases, as well as for other established plasminogen binding enolases (Table S2). This motif is commonly composed by positively and negatively charged residues, flanked by hydrophobic residues. Interestingly, the seven enzymatically competent enolases, might also be capable of binding plasminogen according to the conservation of the motif. That is not the case of enolases encoded by TVAG_170370 and TVAG_148010.

3.3.3. Analysis of host extracellular RNA (exRNA) binding site

Recently, extracellular enolase was identified as a novel host derived exRNA-binding protein on *S. pneumoniae* surface, and six enolase exRNA-binding sites were characterized (^{59}RYGGLGTQK^{67}, ^{104}KGKLGA^{109}, ^{188}HALKKILKSRGLETA^{202}, ^{312}GKKVQL^{317}, ^{401}RTDRIAK^{408} and ^{432}LKK^{434}) [47]. ExRNA has been detected in bodily fluids such as urine, semen, menstrual blood, and vaginal fluid [48,49]. Therefore, we analyzed the possible exRNA binding sites within *T. vaginalis* enolases. Again, enzymatically and plasminogen-binding competent enolases (encoded by TVAG_464170, TVAG_043500, TVAG_329,460, TVAG_358110, TVAG_263740, TVAG_487600, TVAG_282090), show five (out of six) of these binding motifs highly conserved. Particularly, they harbor several positive (lysine and arginine) aminoacid residues, which might be important for interaction with exRNA. On the contrary the C-terminal site, containing lysine 434 is not found in *T. vaginalis* enolase. Therefore, although it has still to be experimentally confirmed, there is a possibility that *T. vaginalis* enolase might be able of interacting with host derived exRNA, and thus contributing to *T. vaginalis* infection, signifying that further investigation is required.

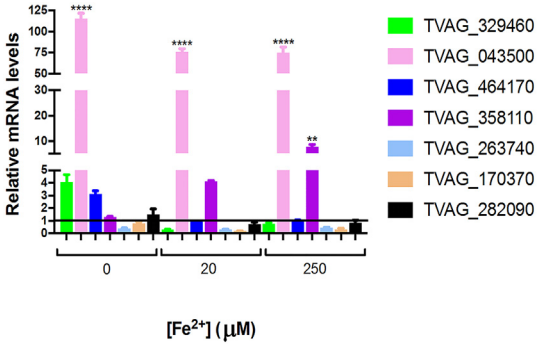

Fig. 4. Quantitative determination of the expression of enolase genes from *T. vaginalis* and its dependence on iron concentration measured by qRT-PCR. All measurements are shown relative to the expression levels of TVAG_464170 at normal iron concentration conditions. β-Tubulin was used as internal control. Data were analyzed using One-way ANOVA. Values are means ± SD ($n = 3$) $p < 0.06$ versus control.

3.4. Enolase genes have different expression levels

The expression of each enolase gene was assessed by two different approaches; we measured RNA levels by RT-PCR experiments and we performed SDS-PAGE and 2-DE experiments to assess the expression of enolase on the isolate CNCD-147, which has been subject of thorough molecular characterization by our research group.

4. 3.5 mRNA levels

A hallmark on the metabolism of *Trichomonas vaginalis*, is the dependence of the expression of several genes on the iron concentration within the culture-media. We analyzed the mRNA levels of enolase genes and their dependence of iron abundance in the culture media (Fig. 4) in CNCD-147 isolate. The gene corresponding to TVAG_487600, was not amplified, even though a wide range of experimental conditions were assayed. Therefore, this description comprehends the other seven enolase genes from *T. vaginalis*. Fold changes in mRNA levels (mean ± SD) are expressed relative to enolase gene TVAG_464170, under normal iron conditions; since the product of this gene has the highest number of ESTs reports (Table S1).

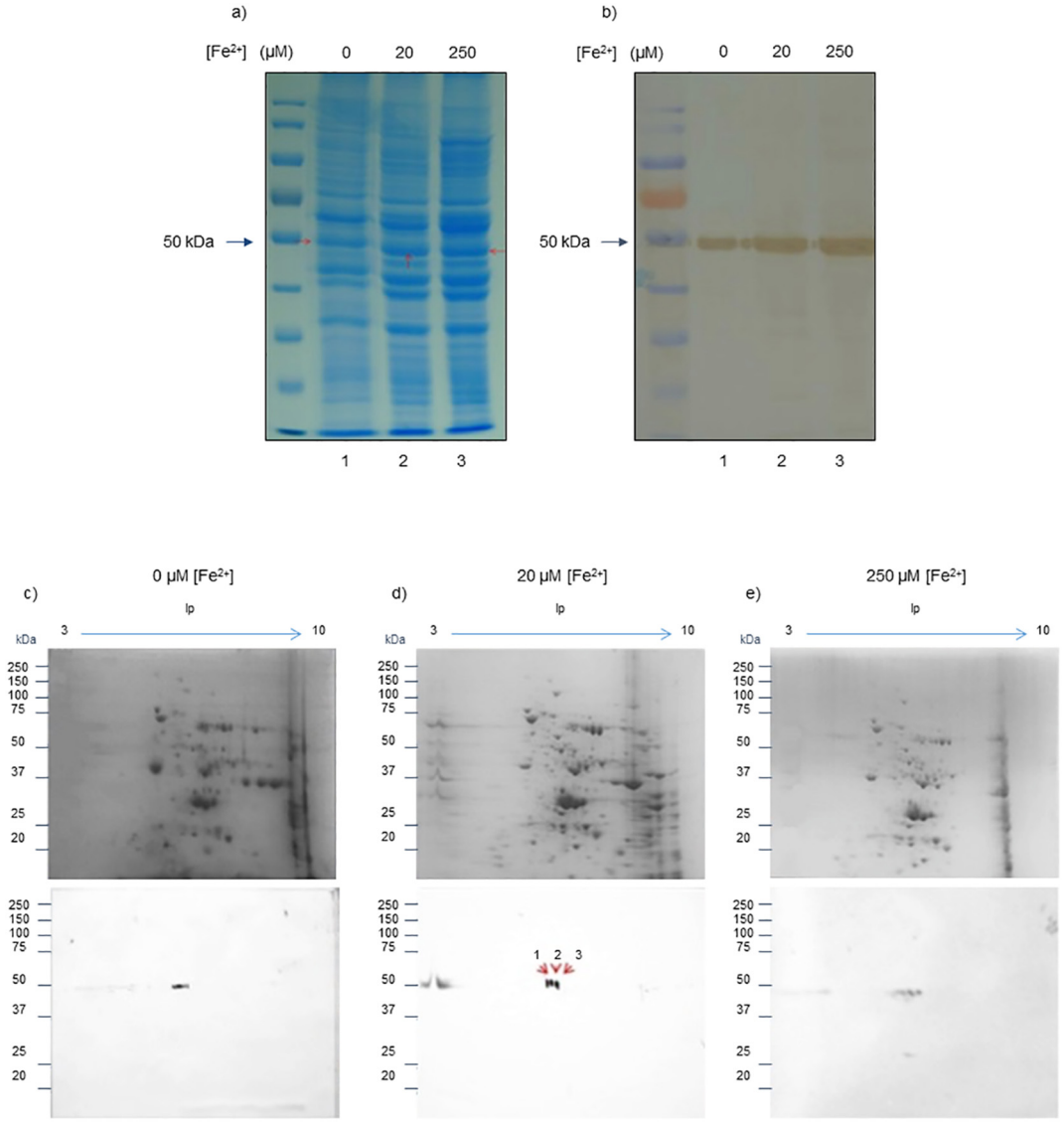

Fig. 5. Analysis of the expression of enolases from *T. vaginalis*. a) SDS-PAGE and b) Western Blot, of protein total extracts from *T. vaginalis*; iron concentration is indicated in each lane. c), d) and e) 2-DE and Western Blot, for c) low, d) normal and e) high iron concentration conditions.

In general, we observed that the enolase gene with highest mRNA levels was TVAG_043500, under all three iron concentration conditions. mRNA levels for this gene are very similar in normal and iron rich cultures (73.9 and 78.1 fold change, respectively), and higher in iron depleted cultures (118.3 fold change). TVAG_358110 occupies the second place of mRNA levels at normal and high concentrations of iron (4.2 and 8.1 fold change respectively), whereas the expression is less abundant in low iron concentration conditions (1.3 fold change). On the opposite, *Trichomonas vaginalis* grown at normal and high iron concentration contain very low levels of genes corresponding to TVAG_263740, TVAG_170370, TVAG_282090, TVAG_464170 and TVAG_329460.

Interestingly, several enolase genes (TVAG_043500, TVAG_329460, TVAG_464170, TVAG_282090 and TVAG_170370) are upregulated when parasites were grown using iron depleted cultures. Furthermore, genes corresponding to TVAG_358110, TVAG_263740 and TVAG_464170, show highest mRNA levels at iron rich conditions.

4.1. Proteomics approach

We carried out SDS-PAGE, 2-DE and Western Blot analysis of total protein extracts to detect the enolase on *T. vaginalis* grown at three different iron concentrations (rich, normal and iron depleted). Three spots were resolved with molecular weight ranging from 51 to 53 kDa and pI from 5.7 to 6.6, which might be attributed to enolases, as judged from recognition with antibody anti-enolase (Fig. 5). Proteins were identified by MaldiToF Mass spectrometry. In Table S3, we show the peptides identified in each case. In the case of spots marked with numbers one and two, we obtained peptides corresponding to the products of either TVAG_043500 or TVAG_329,460, therefore, from the sequence of peptides it is not possible to discriminate between these proteins. Nevertheless, according to isoelectric points, it is plausible to propose that spot marked with number one, corresponds to TVAG_329,460, while spot number two belongs to TVAG_043500. In the case of the spot marked with number three, some of the peptides found are harbored exclusively in enolase encoded by TVAG_464170. The results were similar in all iron concentration conditions.

5. Discussion

Enolase from *Trichomonas vaginalis* is a moonlighting protein that apart from the canonic participation in glycolysis, also acts as a plasminogen receptor on the surface of the parasite, and in consequence, it has been described as a new surface-associated virulence factor. Here we performed a molecular characterization of each of the nine genes encoding for this protein, as well as their expression patterns.

All nine contigs annotated as enolase in TrichDB (www.trichdb.org) are independent form each other, since they all are in different contigs.

Seven enolases (encoded by TVAG_464170, TVAG_043500, TVAG_329460, TVAG_358110, TVAG_263740, TVAG_487600 and TVAG_282090) are competent of performing enzymatic activity, since they harbor the majority of the aminoacid residues of the catalytic moiety, as well as divalent cation binding site residues reported for enolases from other organisms [7,34,36]. Interestingly the same seven enolases are also prone to bind plasminogen. These results argue against the hypothesis that some members of the enolase family could bind plasminogen and others could have enzyme activity. In addition, the same group also harbor host derived exRNA-binding motifs. To confirm the functional plasticity of these enolases further studies are needed.

Furthermore, phylogenetic reconstruction showed that the same set of seven enolases, might have derived from a common ancestor, and were grouped together, among them; the products of three genes (TVAG_464170, TVAG_043500, TVAG_329460) are the most closely related.

Regarding the other two enolases, (corresponding to genes TVAG_148010 and TVAG_170370), might either be pseudogenes or might perform a different function within the parasite, but they are not competent to perform neither enzymatic activity, nor plasminogen binding; since they lack the functional moieties. In addition, they are the most distinctly related members of the family.

Furthermore, we analyzed the expression of enolase genes within the highly virulent mexican strain CNCD-147 at different iron concentration conditions using qRT-PCR and proteomics techniques.

We could detect the amplification of all enolase genes except for TVAG_487600, although we tested several experimental conditions. Furthermore, we observed that for most enolase genes mRNA levels decrease with iron concentration, the highest exception is TVAG_358110. On the contrary, other authors have reported down regulation in iron depleted conditions (TVAG_464170, −2.65 fold change and TVAG_043500, −14.3 fold change) [50]. In comparison, the highest number of ESTs reports is for TVAG_464170, followed by TVAG_043500, TVAG_358110 and TVAG_329460 in third and fourth place, respectively. Nevertheless, all condition tested in ESTs reports are with different strains and culture conditions to those used in this study.

The highest levels of mRNA in all concentration conditions were detected for TVAG_043500. The second place is occupied by TVAG_329460 and TVAG_358110 at low or normal and high iron concentrations, respectively. mRNA relative levels of TVAG_464170 occupy the third place in abundance, in all conditions tested. The rest of enolases show very low mRNA levels.

Respect to the proteomics approach, three protein spots could be resolved and identified by antibody anti-enolase. Only one enolase could be unequivocally detected (TVAG_464170) in all iron concentration conditions. The other two spots provided the same peptides which match with two enolases (TVAG_043500 and TVAG_329460), which might be differentiated by their theoretical isoelectric points. Although TVAG_358110 show high mRNA levels at normal and high iron concentration conditions, it could not be detected by mass spectrometry analysis. *Cis*-regulatory elements of this gene do not show any evident difference in comparison with those genes that could be detected by the proteomics approach.

In particular, finding the product of TVAG_329460 is interesting since it has been encountered on the cell surface of B7RC2 strain (PA strain, ATCC 50167) [13] [51], and additionally it has been probed to perform the moonlighting activity as plasminogen receptor on the cell surface of T016 strain [6], and therefore, described as a new surface-associated virulence factor. Although, as it has been mentioned, seven enolases are prone to perform plasminogen-binding activity, and in other *T. vaginalis* strains TVAG_464170 and TVAG_358110 have been detected in cytoadherence [15] [52] conditions, as well as in the surface proteome [13].

The genes corresponding to TVAG_263740, TVAG_487600, TVAG_282090, TVAG_170370, and TVAG_148010 seem to be the less expressed, and undetectable by proteomics approach. In comparison, in other *T. vaginalis* strains, and experimental conditions, they show very few or null EST's reports [4].

5.1. Discrepancy between mRNA levels and proteomic analysis

We studied the expression of eight enolase genes from CNCD-147 isolate of *Trichomonas vaginalis*, by means of measuring relative mRNA levels and proteomic analysis, under three experimental conditions, varying the iron concentration of culture media. We observed some contrasting results between the two approaches. This lack of correlation has also been reported in a wide number of cases, and has been attributed to a set of post-transcriptional (including mRNA degradation), translational (rates of protein production, protein folding) and protein degradation (protein stability, and in vivo half-life of proteins) events constitutively/intrinsically taking place within the cell in order to control steady-state protein abundances, as well as noise and

experimental error, and they are not mutually exclusive. We performed some sequence analyses, in order to try to identify some possible contributors to the lack of correlation between enolase genes mRNA levels and detected proteins by mass-spectrometry. We studied the codon usage of enolase genes from *Trichomonas vaginalis* (data not shown), but we were not able to detect significant differences between the adaptability index among enolase genes. In addition, since PEST (proline, glutamic acid, serine and threonine) motifs reduce the half-lives of proteins, we also analyzed enolases protein-sequences to detect the presence of these motifs (data not shown). We obtained that all enolase proteins display either six (TVAG_464170, TVAG_282090, TVAG_487600, and TVAG_043500) or seven (TVAG_170370, TVAG_329460, TVAG_358110, and TVAG_263740) poor potential putative-PEST. Therefore, neither codon usage, nor PEST-motifs could be associated to the lack of correlation between mRNA levels and proteomics approach results. Furthermore, we also revised the instability index (based on a statistical analysis that revealed that there are certain dipeptides that are more frequently encountered in unstable proteins). Curiously, the lowest instability index was calculated for the product of gene TVAG_464170, the probably constitutively expressed enolase, followed by the product of TVAG_043500. Even if this is a simplistic sequence analysis, in future studies, the stability as well as other physicochemical analyses of each product of enolase genes from *Trichomonas vaginalis* are interesting fields of study, to better understand the structure, and function of this enzyme within the parasite.

5.2. Enolase from T. vaginalis as a drug or vaccine target

Enolase as a multifunctional protein has been involved in cellular stress, bacterial and fungal infections, autoantigen activities, the occurrence and metastasis of cancer, parasitic infections, and the growth, development and reproduction of organisms. It is also recognized as an important virulence factor among several pathogens [5,53,54]. Consequently, both glycolytic and non-glycolytic functions of enolase have been utilized to design novel therapeutic strategies for a wide variety of physiopathologies. One of the best examples of succes is the use of the small molecule depicted as ENOblock, which binds enolase and modulates its non-glycolytic “moonlighting” functions [14]. ENOblock treatment on a mammalian model of type 2 diabetes mellitus, reduced hyperglycemia and hyperlipidemia, and produced beneficial effects on lipid homeostasis, fibrosis, inflammatory markers, nephrotoxicity and cardiac hypertrophy.

The active site In *T. vaginalis*, shows three key substitutions (K157(159)S, G161(163)N and N162(164)K), when compared to human enolase, these differences might be considered as potential inhibitor targets, and deserve further studies.

In addition, enolase has been detected on the surface of several organisms, but the precise mechanism through enolase reaches and stays on the cell surface is still to be fully determined, since this protein does not have signal sequences nor membrane-anchoring motifs [55,56,57]. Enolase has also been detected on the surface of *T. vaginalis*, and its ability to bind plasminogen has been confirmed [6].

We found that the most relevant feature observed in the sequences all enolases from *Trichomonas vaginalis* is that they contain unique N-terminal regions ranging from 35 to 63 aminoacid residues that are not encountered in enolases from other organisms, and that do not show sequence similarity with any other reported mammal protein-sequence as judged from blast analysis. The function of this unique region still needs to be explored. Nevertheless, we could detect that for the seven enzymatically and plasminogen-binding competent enolases, the unique N-terminal extension displays a common motif. This motif involves 15-18 aminoacid residues, which consensus sequence is $BXEDN_pN_pGXLS(L/I)(L/F)(X)_{0-2}(B)_{1-3}AN_p$. Where B, corresponds to a basic aminoacid; X could be any aminoacid, polar or non- polar; Np, stands for a non-polar residue. The function and conformational relevance of this unique region within enolase from *T. vaginalis* needs to be determined. Indeed, future in-depth studies are necessary, but this unique N-terminal region represents an attractive target for drug and vaccine design as well as diagnostic marker to fight trichomonosis.

6. Concluding remarks

T. vaginalis is characterized by multiple gene copies. It is believed, that this multiplicity provides to this parasite the capability of adapting to environmental changes where trophozoites grow. In addition, *T. vaginalis* strains or isolates show variable degree of virulence, adhesion capacity and drug resistance. These phenotypes certainly might depend on the expression of many proteins, involving enolase. We found that seven out of nine enolase genes annotated in TrichDB, are closely related and should have been derived from a common ancestor. Furthermore, the seven related genes contain the cis promoter elements in 5′and 3′UTR sequences, commonly observed in expressed genes in *T. vaginalis*. Furthermore, we found that the products of these seven genes contain functional domains, for performing both enzymatic activity and plasminogen binding. The other two genes annotated as enolase, are neither closely related to the rest of the group, neither their products show functional domains, so they might be either pseudogenes, or might perform a different function on parasite cells, if they were expressed. Regarding the expression, we could detect peptides corresponding only to three functional genes, at different iron concentration conditions.

Enolases from *T. vaginalis*, show distinctive sequence characteristics within one of the active site loops and a unique N-terminal region (conserved solely in enolases from this parasite) which in conjunction offer new perspectives for both drug discovery, vaccination and diagnosis against the most common non-viral sexually transmitted disease trichomonosis.

Supplementary data to this article can be found online at https://doi.org/10.1016/j.parint.2018.04.003.

Funding information

We thank financial support from Fondo Sectorial de Innovación Secretaría de Economía-CONACyT (FINNOVA), Bonos para la Innovación, grant Number "216767 “Desarrollo de Fármacos para el tratamiento de la infección de transmisión sexual Tricomoniasis, Fase Preclínica”, SIP-IPN grants 20140317, 20150391 and 20160239. ICYT-DF grants PICSA 10-19. Beca de Estudios de Doctorado CONACyT No. 263610/226088.

Ethics

Authors attest that this article is original and they agree with the publication of the manuscript without any ethical issues involved.

Acknowledgements

We thank to Departamento de Bioquímica Estructural, CINVESTAV, Unidad Irapuato and Departamento de Infectómica y Patogénesis Molecular CINVESTAV, Unidad Zacatenco for permitting the use of their research laboratory. We acknowledge grateful the assistance of M.Sc. Alicia Chagolla for helping in the analysis and identification of proteins by Matrix assisted lasser desorption/ionization (MALDI)- time of Fligth (TOF) from Departamento de Biotecnología y Bioquímica CINVESTAV, Unidad Irapuato.

References

[1] L. Newman, et al., Global estimates of the prevalence and incidence of four curable sexually transmitted infections in 2012 based on systematic review and global reporting, PLoS One 10 (12) (Dec. 2015) e0143304.
[2] D. Leitsch, Recent advances in the *Trichomonas vaginalis* field, F1000Res. 5 (162)

(Feb. 2016) 1–7 (F1000 Faculty Rev).
[3] S.-B. Malik, et al., Phylogeny of parasitic Parabasalia and free-living relatives inferred from conventional markers vs. Rpb1, a single-copy gene, PLoS One 6 (6) (Jun. 2011) e20774.
[4] S. Singh, et al., Insight into *Trichomonas vaginalis* genome evolution through metabolic pathways comparison, Bioinformation 8 (4) (Feb. 2012) 189–195.
[5] A. Diaz-Ramos, A. Roig-Borrellas, A. Garcia-Melero, R. Lopez-Alemany, alpha-Enolase, a multifunctional protein: its role on pathophysiological situations, J Biomed Biotechnol 2012 (2012) 156795.
[6] V. Mundodi, A.S. Kucknoor, J.F. Alderete, Immunogenic and plasminogen-binding surface-associated alpha-enolase of *Trichomonas vaginalis*, Infect. Immun. 76 (2) (Feb. 2008) 523–531.
[7] H.J. Kang, S.-K. Jung, S.J. Kim, S.J. Chung, Structure of human alpha-enolase (hENO1), a multifunctional glycolytic enzyme, Acta Crystallogr. D. Biol. Crystallogr. 64 (Pt 6) (Jun. 2008) 651–657.
[8] V. Pancholi, Multifunctional alpha-enolase: its role in diseases, Cell. Mol. Life Sci. 58 (7) (Jun. 2001) 902–920.
[9] P. Mangalam, V. Vasuki, R. Balasubramaniyan, Enolase in vector-borne pathogens: a potential therapeutic target, J. Entomol. Zool. Stud. 4 (5) (2016) 699–709.
[10] W. Jiang, et al., Identification and characterization of an immunogenic antigen, enolase 2, among excretory/secretory antigens (ESA) of *Toxoplasma gondii*, Protein Expr. Purif. 127 (Nov. 2016) 88–97.
[11] N. Salazar, M.C.L. de Souza, A.G. Biasioli, L.B. da Silva, A.S. Barbosa, The multifaceted roles of *Leptospira* enolase, Res. Microbiol. 168 (2) (Feb. 2017) 157–164.
[12] L. Avilán, et al., Enolase: a key player in the metabolism and a probable virulence factor of trypanosomatid parasites-perspectives for its use as a therapeutic target, Enzym. Res. 2011 (2011) 932549.
[13] N. de Miguel, G. Lustig, O. Twu, A. Chattopadhyay, J.A. Wohlschlegel, P.J. Johnson, Proteome analysis of the surface of *Trichomonas vaginalis* reveals novel proteins and strain-dependent differential expression, Mol. Cell. Proteomics 9 (7) (Jul. 2010) 1554–1566.
[14] H. Cho, et al., ENOblock, a unique small molecule inhibitor of the non-glycolytic functions of enolase, alleviates the symptoms of type 2 diabetes, Sci. Rep. 7 (Mar. 2017) 44186.
[15] J.M. Carlton, et al., Draft genome sequence of the sexually transmitted pathogen *Trichomonas vaginalis*, Science 315 (5809) (Jan. 2007) 207–212.
[16] C. Aurrecoechea, et al., GiardiaDB and TrichDB: integrated genomic resources for the eukaryotic protist pathogens *Giardia lamblia* and *Trichomonas vaginalis*, Nucleic Acids Res. 37 (Database) (Jan. 2009) D526–D530.
[17] M. Gouy, S. Guindon, O. Gascuel, SeaView version 4: a multiplatform graphical user interface for sequence alignment and phylogenetic tree building, Mol. Biol. Evol. 27 (2) (Feb. 2010) 221–224.
[18] R.C. Edgar, MUSCLE: multiple sequence alignment with high accuracy and high throughput, Nucleic Acids Res. 32 (5) (2004) 1792–1797.
[19] S. Guindon, J.-F. Dufayard, V. Lefort, M. Anisimova, W. Hordijk, O. Gascuel, New algorithms and methods to estimate maximum-likelihood phylogenies: assessing the performance of PhyML 3.0, Syst. Biol. 59 (3) (Mar. 2010) 307–321.
[20] P.D. Schloss, Application of a database-independent approach to assess the quality of operational taxonomic unit picking methods, mSystems 1 (2) (Apr. 2016).
[21] M.R. Mendoza-López, et al., CP30, a cysteine proteinase involved in *Trichomonas vaginalis* cytoadherence, Infect. Immun. 68 (9) (Sep. 2000) 4907–4912.
[22] V. Pancholi, V.A. Fischetti, α-Enolase, a novel strong plasmin(ogen) binding protein on the surface of pathogenic *Streptococci*, J. Biol. Chem. 273 (23) (Jun. 1998) 14503–14515.
[23] J.B. De Jesus, et al., Application of two-dimensional electrophoresis and matrix-assisted laser desorption/ionization time-of-flight mass spectrometry for proteomic analysis of the sexually transmitted parasite Trichomonas vaginalis, J. Mass Spectrom. 42 (11) (Nov. 2007) 1463–1473.
[24] M. Garcia-Flores, et al., Evaluating the physiological state of maize (Zea mays L.) plants by direct-injection electrospray mass spectrometry (DIESI-MS), Mol. BioSyst. 8 (6) (Jun. 2012) 1658–1660.
[25] T.D. Schmittgen, K.J. Livak, Analyzing real-time PCR data by the comparative C(T) method, Nat. Protoc. 3 (6) (2008) 1101–1108.
[26] A.J. Smith, et al., Novel core promoter elements and a cognate transcription factor in the divergent unicellular eukaryote *Trichomonas vaginalis*, Mol. Cell. Biol. 31 (7) (Apr. 2011) 1444–1458.
[27] A. Smith, P. Johnson, Gene expression in the unicellular eukaryote *Trichomonas vaginalis*, Res. Microbiol. 162 (6) (Jul. 2011) 646–654.
[28] V. Fuentes, G. Barrera, J. Sánchez, R. Hernández, I. López-Villaseñor, Functional analysis of sequence motifs involved in the polyadenylation of *Trichomonas vaginalis* mRNAs, Eukaryot. Cell 11 (6) (Jun. 2012) 725–734.
[29] N. Espinosa, R. Hernández, L. López-Griego, I. López-Villaseñor, Separable putative polyadenylation and cleavage motifs in *Trichomonas vaginalis* mRNAs, Gene 289 (1–2) (May 2002) 81–86.
[30] S.F. Altschul, W. Gish, W. Miller, E.W. Myers, D.J. Lipman, Basic local alignment search tool, J. Mol. Biol. 215 (3) (Oct. 1990) 403–410.
[31] M. Remmert, A. Biegert, A. Hauser, J. Söding, HHblits: lightning-fast iterative protein sequence searching by HMM-HMM alignment, Nat. Methods 9 (2) (Dec. 2011) 173–175.
[32] R.S. Coyne, et al., Refined annotation and assembly of the *Tetrahymena thermophila* genome sequence through EST analysis, comparative genomic hybridization, and targeted gap closure, BMC Genomics 9 (1) (2008) 562.
[33] T.M. Larsen, J.E. Wedekind, I. Rayment, G.H. Reed, A carboxylate oxygen of the substrate bridges the magnesium ions at the active site of enolase: structure of the yeast enzyme complexed with the equilibrium mixture of 2-phosphoglycerate and phosphoenolpyruvate at 1.8 A resolution, Biochemistry 35 (14) (Apr. 1996) 4349–4358.
[34] E.C. Schulz, M. Tietzel, A. Tovy, S. Ankri, R. Ficner, Structure analysis of *Entamoeba histolytica* enolase, Acta Crystallogr. D. Biol. Crystallogr. 67 (Pt 7) (Jul. 2011) 619–627.
[35] S. Ehinger, W.-D. Schubert, S. Bergmann, S. Hammerschmidt, D.W. Heinz, Plasmin (ogen)-binding alpha-enolase from *Streptococcus pneumoniae*: crystal structure and evaluation of plasmin(ogen)-binding sites, J. Mol. Biol. 343 (4) (Oct. 2004) 997–1005.
[36] B. Stec, L. Lebioda, Refined structure of yeast apo-enolase at 2.25 A resolution, J. Mol. Biol. 211 (1) (Jan. 1990) 235–248.
[37] J.M. Brewer, C.V.C. Glover, M.J. Holland, L. Lebioda, Enzymatic function of loop movement in enolase: preparation and some properties of H159N, H159A, H159F, and N207A enolases, J. Protein Chem. 22 (4) (May 2003) 353–361.
[38] J.M. Brewer, J.E. Wampler, A differential scanning calorimetric study of the effects of metal ions, substrate/product, substrate analogues and chaotropic anions on the thermal denaturation of yeast enolase 1, Int. J. Biol. Macromol. 28 (3) (Mar. 2001) 213–218.
[39] T. Lin, M.J. Kornblatt, The binding of Na(+) to apo-enolase permits the binding of substrate, Biochim. Biophys. Acta 1476 (2) (Feb. 2000) 279–286.
[40] P.A. Sims, T.M. Larsen, R.R. Poyner, W.W. Cleland, G.H. Reed, Reverse protonation is the key to general acid-base catalysis in enolase, Biochemistry 42 (27) (Jul. 2003) 8298–8306.
[41] S. Bao, et al., Mycoplasma synoviae enolase is a plasminogen/fibronectin binding protein, BMC Vet. Res. 10 (2014) 223.
[42] S. Bergmann, H. Schoenen, S. Hammerschmidt, The interaction between bacterial enolase and plasminogen promotes adherence of *Streptococcus pneumoniae* to epithelial and endothelial cells, Int. J. Med. Microbiol. 303 (8) (Dec. 2013) 452–462.
[43] V. Vastano, et al., Identification of binding sites of *Lactobacillus plantarum* enolase involved in the interaction with human plasminogen, Microbiol. Res. 168 (2) (Feb. 2013) 65–72.
[44] A. Derbise, Y.P. Song, S. Parikh, V.A. Fischetti, V. Pancholi, Role of the C-terminal lysine residues of *streptococcal* surface enolase in Glu- and Lys-plasminogen-binding activities of group A streptococci, Infect. Immun. 72 (1) (Jan. 2004) 94–105.
[45] A.J. Cork, et al., Defining the structural basis of human plasminogen binding by *streptococcal* surface enolase, J. Biol. Chem. 284 (25) (Jun. 2009) 17129–17137.
[46] M. Candela, et al., Bifidobacterial enolase, a cell surface receptor for human plasminogen involved in the interaction with the host, Microbiology 155 (Pt 10) (Oct. 2009) 3294–3303.
[47] D. Zakrzewicz, et al., Host-derived extracellular RNA promotes adhesion of *Streptococcus pneumoniae* to endothelial and epithelial cells, Sci. Rep. 6 (1) (Dec. 2016).
[48] O.E. Bryzgunova, P.P. Laktionov, Extracellular nucleic acids in urine: sources, structure, diagnostic potential, Acta Nat. 7 (3) (Sep. 2015) 48–54.
[49] E.K. Hanson, H. Lubenow, J. Ballantyne, Identification of forensically relevant body fluids using a panel of differentially expressed microRNAs, Anal. Biochem. 387 (2) (Apr. 2009) 303–314.
[50] N.C. Beltrán, et al., Iron-induced changes in the proteome of *Trichomonas vaginalis* hydrogenosomes, PLoS One 8 (5) (May 2013) e65148.
[51] K.-Y. Huang, et al., A proteome reference map of *Trichomonas vaginalis*, Parasitol. Res. 104 (4) (Mar. 2009) 927–933.
[52] K.-Y. Huang, P.-J. Huang, F.-M. Ku, R. Lin, J.F. Alderete, P. Tang, Comparative transcriptomic and proteomic analyses of *Trichomonas vaginalis* following adherence to fibronectin, Infect. Immun. 80 (11) (Nov. 2012) 3900–3911.
[53] S. Bergmann, M. Rohde, G.S. Chhatwal, S. Hammerschmidt, alpha-Enolase of *Streptococcus pneumoniae* is a plasmin(ogen)-binding protein displayed on the bacterial cell surface, Mol. Microbiol. 40 (6) (Jun. 2001) 1273–1287.
[54] A.K. Ghosh, M. Jacobs-Lorena, Surface-expressed enolases of *Plasmodium* and other pathogens, Mem. Inst. Oswaldo Cruz 106 (Suppl. 1) (Aug. 2011) 85–90.
[55] A. Jolodar, P. Fischer, S. Bergmann, D.W. Büttner, S. Hammerschmidt, N.W. Brattig, Molecular cloning of an alpha-enolase from the human filarial parasite *Onchocerca volvulus* that binds human plasminogen, Biochim. Biophys. Acta 1627 (2–3) (Jun. 2003) 111–120.
[56] A.Y. Jong, Binding of *Candida albicans* enolase to plasmin(ogen) results in enhanced invasion of human brain microvascular endothelial cells, J. Med. Microbiol. 52 (8) (Aug. 2003) 615–622.
[57] D. Bernal, J.E. de la Rubia, A.M. Carrasco-Abad, R. Toledo, S. Mas-Coma, A. Marcilla, Identification of enolase as a plasminogen-binding protein in excretory-secretory products of *Fasciola hepatica*, FEBS Lett. 563 (1–3) (Apr. 2004) 203–206.